Study of multinucleon knockout reactions of exotic nuclei in the region of Sn

M. Feijoo-Fontán[1*], *E.* Kudaibergenova[2], *I.* Lihtar[3], *I.* Gasparic[3], *A.* Horvat[2,3], *J.L.* Rodriguez-Sanchez[1], *V.* Panin[4], *H.* Alvarez-Pol[1], *L.* Atar[2], *T.* Aumann[2,4,5], *J.* Benlliure[1], *K.* Boretzky[4], *M.J.G.* Borge[6], *L.T.* Bott[7], *C.* Caesar[4], *E.* Casarejos[8], *J.* Cederkall[9], *A.* Chatillon[10], *D.* Cortina-Gil[1], *E.* De Filippo[11], *T.* Dickel[4], *M.* Duer[2], *A.* Falduto[2], *D.* Galaviz[12], *G.* García-Jiménez[1], *Z.* Ge[4], *E.I.* Geraci[11,13], *R.* Gernhäuser[14], *B.* Gnoffo[11,13], *A.* Graña-González[1], *K.* Göbel[7], *E.* Haettner[4], *A.L.* Hartig[2], *M.* Heil[4], *A.* Heinz[15], *T.* Hensel[16], *M.* Holl[15], *C.* Hornung[4], *A.* Jedele[2], *D.* Jelavic-Malenica[2], *T.* Jenegger[14], *L.* Ji[2], *H.T.* Johansson[15], *N.* Kalantar-Nayestanaki[17], *E.* Kazantseva[4], *A.* Kelić-Heil[4], *O.A.* Kiselev[4], *P.* Klenze[4,14], *R.* Knoebel[4], *D.* Körper[4], *T.* Kröll[2], *B.* Löher[4], *N.S.* Martorana[18], *L.* Milhomens da Fonseca[2], *P.* Morfouace[10], *I.* Mukha[4], *S.* Murillo-Morales[19], *E.* Nácher[6], *C.* Nociforo[4], *A.* Obertelli[2], *S.* Paschalis[19], *A.* Perea[6], *M.* Petri[19], *S.* Pietri[4], *S.* Pirrone[11], *L.* Ponnath[14], *H.B.* Rhee[2], *L.* Rose[19], *D.M.* Rossi[2,4], *P.* Russotto[18], *D.* Savran[4], *C.* Scheidenberger[4], *H.* Simon[4], *J.P.* Simon[2], *S.* Storck-Dunite[2], *A.* Stott[19], *Y.* Sun[2], *D.* Symochko[2], *C.* Sürder[2], *J.* Taïeb[10], *R.* Taniuchi[19], *O.* Tengblad[6], *H.T.* Törnqvist[2,4], *S.* Velardita[2], *F.* Wamers[4], *H.* Weick[4], *J.* Zhao[4], and the R^{3}B collaboration

[1]IGFAE, Universidade de Santiago de Compostela, E-15782 Santiago de Compostela, Spain
[2]Technische Universität Darmstadt, Fachbereich Physik, Institut für Kernphysik, 64289 Darmstadt, Germany
[3]RBI Zagreb, Bijenicka cesta 54, HR10000, Zagreb, Croatia
[4]GSI Helmholtzzentrum für Schwerionenforschung, Planckstraße 1, 64291, Darmstadt, Germany
[5]Helmholtz Research Academy Hesse for FAIR, 64289 Darmstadt, Germany
[6]Instituto de Estructura de la Materia, CSIC, E-28006 Madrid, Spain
[7]Goethe-Universität Frankfurt, Max-von-Laue Str. 1, 60438, Frankfurt am Main, Germany
[8]CINTECX, Universidade de Vigo, E-36200 Vigo, Spain
[9]Department of Physics, Lund University, P.O. box 118, 221 00 Lund, Sweden
[10]CEA, DAM, DIF, F-91297 Arpajon, France
[11]INFN Sezione di Catania, Via Santa Sofia 64, 95123, Catania, Italy
[12]Laboratório de Instrumentação e Física Experimental de Partículas, LIP, Av. Prof. Gama Pinto 2, 1649-003 Lisbon, Portugal
[13]Università di Catania, Dipartimento di Fisica e Astronomia "Ettore Majorana", Catania, Italy
[14]Technische Universität München, James-Franck-Str 1, 85748, Garching, Germany
[15]Institutionen för Fysik, Chalmers Tekniska Högskola, 412 96 Göteborg, Sweden
[16]Helmholtz-Zentrum Dresden-Rossendorf, Institute of Radiation Physics, Bautzner Landstraße 400, 01328, Dresden, Germany
[17]ESRIG, University of Groningen, Groningen, Netherlands
[18]INFN Laboratori Nazionali del Sud, Via Santa Sofia 62, 95133, Catania, Italy
[19]School of Physics, Engineering and Technology, University of York, YO10 5DD York, UK

Abstract. The experimental data collected during the S515 experiment performed by the R^{3}B collaboration at GSI/FAIR represent a great opportunity to investigate nucleon knockout reactions of exotic nuclei in the region of Sn using complete kinematics measurements. These cross sections can be used in the future to investigate the quenching in the knockout of the minority species (neutrons or protons) in nuclei far from stability. Some of the arguments put forward are the underestimation of the knockout of deeply bound nucleons, final state interactions or the role of short-range correlations (SRC). Recently, several works based on inclusive measurements have shown that these SRCs could reduce the single nucleon knockout cross sections by around 50%, depending on the neutron excess (N/Z) of the initial projectile. The S515 data can help us to go further in this investigation because it allows to correlate the knockout cross sections of one, two or more nucleons with the number of protons and neutrons emitted from the target and which can be detected by the CALIFA and NeuLAND detectors, respectively, and perform complete kinematical studies on the nature of the event (SRC, evaporation, emission of clusters, final-state interactions...). Here the results obtained for the charge distribution of reaction residues are presented, which is one of the first steps of the still on-going analysis.

1 Introduction

Knockout reactions offer a powerful tool for identifying the single-particle structure of nuclei since they are direct nucleon-nucleon collisions of the probe particles with the shell nucleons. In particular, one of the objects of study can be the determination of spectroscopic factors, i. e., how much the independent particle model (IPM) is fulfilled in reality. A significant deviation from IPM model that seemed independent from the asymmetry parameter ΔS defined as $S_n - S_p$ ($S_p - S_n$) for neutron (proton)

*email: *martina.feijoo.fontan@usc.es*

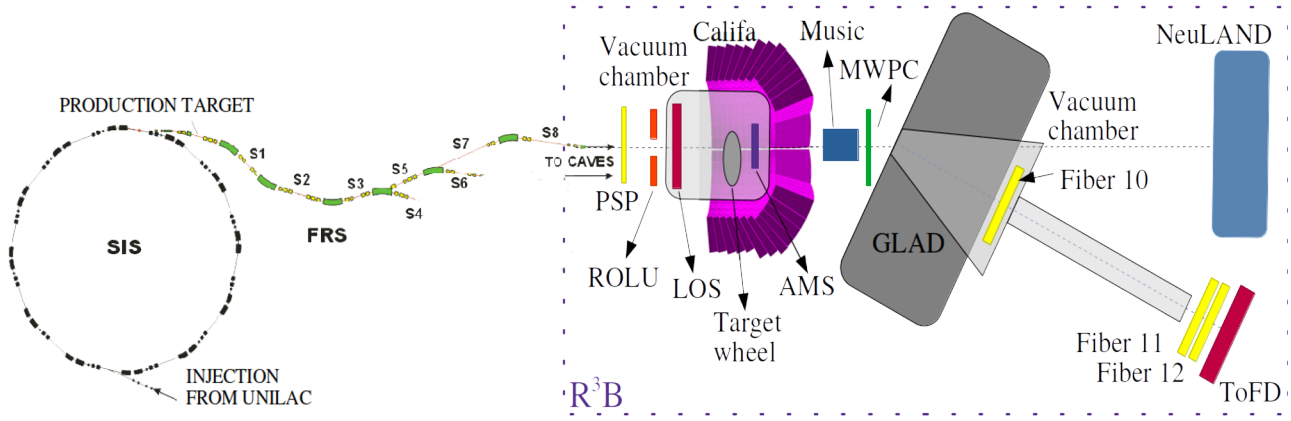

Figure 1. Schematic representation of the experimental setup used in the present work. Sizes are not to scale.

knockout was found [1, 2] both when studying transfer reactions as well as quasi-elastic electron scattering $(e, e'p)$. Nevertheless, experiments performed in inverse kinematics and with composite nuclear targets, such as beryllium and carbon, found a clear dependency between ΔS and the reduction of the experimental cross sections of single nucleon knockout compared to the shell model predictions [3]. Several works, based on inclusive measurements [4, 5] focused on the study of neutron-rich-medium-mass nuclei around Sn, showed that this reduction expressed as dependence on the neutron excess (N/Z) (which can be translated into ΔS) of the initial projectile is more noticeable for proton-removal reactions.

The quenching can be partially explained as an effect of SRC, which are pairs of nucleons having large relative momentum, proton-neutron being the dominant ones [6]. Because of this, the fraction of paired protons is larger than the neutron pairs, in the case of neutron-rich nuclei. In addition, investigations in Refs. [3, 4] indicate that the excitation energy of the remnant nuclei calculated with the current models is underestimated, resulting in a higher probability for particle evaporation after the reaction and reducing the measured fragments associated with the single-knockout channel. Another factor contributing to the overestimation of the core survival probability could be the omission of statistical cascade-model-like processes [7], mainly for weakly-bound cores. Finally, the emission of clusters could also be playing a significant role.

In this experiment the single nucleon knockout (A-1) channel was extended to the multiple ones (A-2, A-3,...). Moreover, the evaporated particles can also be detected, hence this experiment provides for the first time access to complete kinematic information for such reactions. This work will try to study the different contributions of the mentioned factors to the observed quenching in the knockout cross sections. In addition, gamma emission of excited states of Sn isotopes can be measured as well, since an unexpected favored gamma-deexcitation was observed above neutron evaporation threshold [8].

The following outlines the experimental setup briefly. Moreover, the results obtained for the identification of the incoming projectiles, delivered via the fragment separator FRS, and the reaction residues are presented as a function of the atomic number (Z), as well as their production cross sections. These are the first steps of the analysis, which will be continued in order to link the produced fragments and their knocked-out particles with the effects described above.

2 Experiment

The S515 experiment was performed in spring 2021 at GSI, using two different production mechanisms, cocktail beams produced at the entrance of the FRS and guided through the spectrometer to the experimental cave (see Figure 1). The first type of beam was produced from the fragmentation of ^{136}Xe on a Be target, resulting in a secondary beam centered on the isotope ^{124}Sn. This was done at two different beam energies in order to get the secondary beam at 405 and 900 MeV/u in the experimental hall. The second cocktail beam was produced via fission of ^{238}U on two different Pb targets (2386 mg/cm^2, 1542 mg/cm^2), resulting in secondary cocktail beams containing ^{124}Sn at 872 MeV/u and ^{132}Sn 678 MeV/u. With this combination of settings, a wide range of Sn isotopes can be studied using the inverse kinematics technique. Using this method a large momentum in the center of mass is reached and complete kinematic measurements of all the outgoing fragments can be accomplished.

This kind of measurement is performed with the R^{3}B experimental setup shown in the Figure 1. It consists of several detectors. A Position Sensitive Pin diode (PSP) to measure the charge of the incoming particles, a plastic scintillator (ROLU) that works as a veto to make sure only collimated events are recorded. Another plastic scintillator (LOS) is used to determine the Time-of-Flight (ToF) between the central focal plane of the FRS (S2) and the experimental cave before the target wheel. The different materials and thicknesses used as target were: C(1g/cm^2, 2g/cm^2), CH_2 (1g/cm^2, 2g/cm^2) and Pb (980mg/cm^2). Surrounding the target-area the highly segmented (1504 CsI(Tl) crystals) calorimeter CALIFA (CAlorimeter for In-Flight detection of γ-rays and high energy charged pArticles) is placed to measure gammas and light charged par-

ticles [9]. The MUSIC detector (MUlti-Sampling Ionization Chamber) is used for the charge identification of the reaction residues. Mass identification of both incoming and outgoing isotopes is performed using the ΔE-Bρ-ToF technique. Fiber detectors are used to determine the positions for tracking after the target, while ToF is determined from timing information of the TOFD wall [10] and the start detector LOS. The large acceptance superconducting dipole GLAD is placed behind the R^3B target, bending the trajectories of the reaction residues depending on their A/Q. The forward-emitted neutrons are detected in the NeuLAND detector [11].

3 Results

The first step of the analysis is the identification of the isotopes in the cocktail beam as shown in Figure 2 for the fragmentation setting at 900 MeV/u. In the present work only this FRS setting is considered, focusing the study on the case of ^{124}Sn which is indicated in Figure 2. In the future other isotopes will be studied, as well as the fission settings.

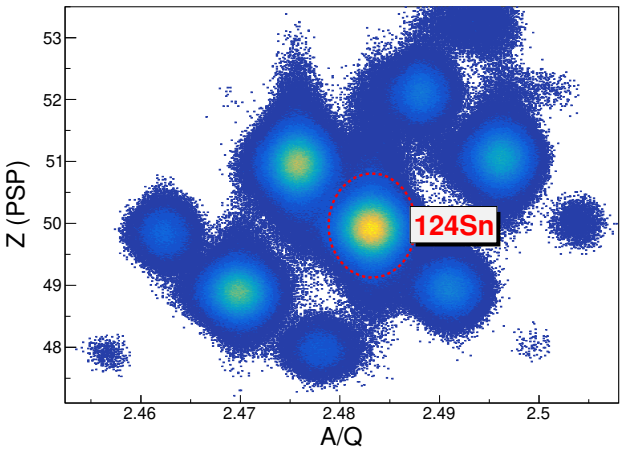

Figure 2. (Color online) Cluster plot displaying the identification of secondary beams in atomic number (Z) and mass-over-charge (A/Q) for an FRS magnetic setting centered on ^{124}Sn.

The charge identification after the target is made, being able to measure a broad range of products with a resolution of 0.48 charge units (FWHM). In Figure 3 the charge distribution is shown for the three different targets when selecting ^{124}Sn as the incoming isotope. The distributions are scaled to equal height at for Z=48, where the electromagnetic excitation contribution is assumed to be negligible. The main difference arises for the Pb target, since the electromagnetic field induced by this element is much larger than for the other two. Because of this, some reaction channels that do not modify the nuclear charge of the projectile and which are not accesible for C, CH_2 targets are open for reaction with a Pb target. Coulomb excitation results, e.g., in an increase of the neutron emission due to the excitation of giant dipole and quadrupole resonances [12]. Consequently, the amount of projectiles that remain with the same charge (Z=50) after the reaction is larger in the case of the lead target. In Figure 3 it can be seen that the difference is of almost one order of magnitude.

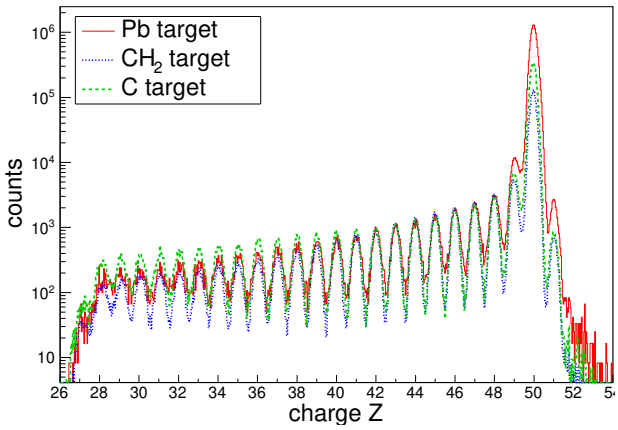

Figure 3. (Color online). Charge distribution comparison of the reaction residues produced by projectiles of ^{124}Sn at 900 MeV/u impinging on C, CH_2 and Pb targets.

Once both identifications are performed, it is possible to determine the charge production cross sections σ_Z for the different targets as follows

$$\sigma_Z = \left(\frac{N_{\text{out}}^{\text{target}}}{N_{\text{in}}^{\text{target}}} - \frac{N_{\text{out}}^{\text{empty}}}{N_{\text{in}}^{\text{empty}}} \right) \frac{M(t)}{d(t) \cdot N_A} \tag{1}$$

where $M(t), d(t)$ are the molar mass and the thickness of the target, respectively, and N_A is Avogadro's number. N_{out} refers to the number of outgoing fragments and N_{in} to the incoming projectiles. Subtracting the number of measured particles from an empty-target measurement ensures that the background is removed, consisting mainly of reactions that occured in matter layers of the setup, such as the scintillators. Finally, a correction regarding secondary reactions in the target is needed. A factor for each target and outgoing charge is calculated utilizing two concatenated simulations: the first one, based on the use of the intranuclear cascade and abrasion reaction models, a distribution of reacted fragments is obtained for ^{124}Sn+p and ^{124}Sn+C. This is the input for the second one, based on Geant4 where the fragments pass through the corresponding material (C, Pb) but considering only half of the length of the target in the experiment. In this way, all secondary reactions are approximated to happen in the center of the target. Afterwards, the correction factors for secondary reactions are calculated as the ratio of incoming over outgoing fragments for each charge. Finally, the cross section obtained from Eq. 1 for each charge is multiplied by the corresponding correction factor. For the measurement with the CH2 target the correction factor is assumed to be the same and is applied to the cross section accordingly.

Preliminary results are shown in Figure 4 for the three targets, considering only statistical uncertainties so far. The proton contribution is obtained as $\sigma_Z^p = 1/2 \cdot (\sigma_Z^{CH_2} - \sigma_Z^C)$. When comparing the results with model calculations, for the two light targets, the INCL (Liège Intranuclear Cascade) model [13, 14] is used, whereas for Pb the calculation is performed using ABRABLA07 [15].

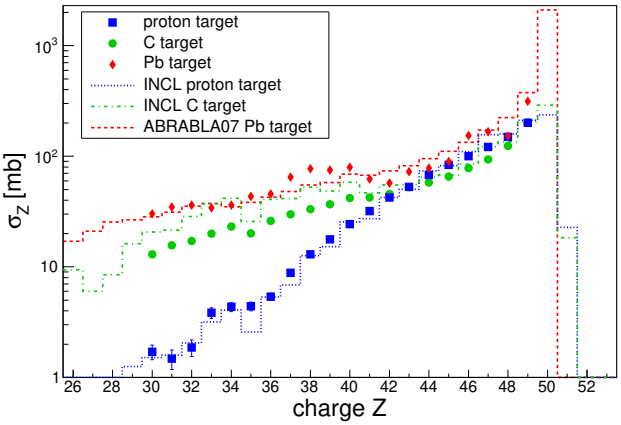

Figure 4. (Color online) Production cross section as a function of the atomic number (Z) measured for ^{124}Sn on p, C and Pb targets. The data are compared to different model calculations.

In general, it can be seen that the obtained experimental production cross sections follow the same trend as the calculated ones. Nevertheless, a further analysis is needed to check for possible mismatches, especially the behaviour found for σ_Z^{Pb} around $Z = 38$ and the sudden decrease visible for $Z = 48$. For the case of σ_Z^C, the reason why the measured values are systematically below those calculated is still not clear.

4 Conclusions and outlook

The fragment separator FRS is combined with the R^{3}B experimental setup to study multi-nucleon knockout reactions of exotic nuclei around Sn. This complex experiment requires the calibration of many detectors in order to identify the incoming and outgoing fragments as well as the emitted particles. In this work we present the first results concerning the charge distribution of reaction residues produced with projectiles of ^{124}Sn impinging onto different targets at kinetic energies of 900 MeV/u. After the detector calibrations, the charge distributions are obtained with a resolution of 0.48 (FWHM). The number of counts for each charge is then corrected by dead times and secondary reactions and normalized to the number of incoming projectiles to obtain the production cross sections. After applying all the corrections the cross sections are obtained with uncertainties smaller than 4% for the direct measurements with the C, CH_2 and Pb targets. For the hydrogen, this uncertainty reaches 19% for the lighter atomic numbers but it is less than 9% for $Z \geq 34$. As expected, the production cross sections of lighter reaction residues increase with the target size, being larger for the Pb target. The data are also compared to INCL+ABLA and ABRABLA07 calculations, showing a reasonable agreement. The next step will be to obtain the cross sections for multi-nucleon knockout channels and extend this investigation to other incoming isotopes.

Additionally, total neutron-removal cross sections could be used to determine the neutron skin thickness and to constrain the slope parameter L of the symmetry energy down to ±10 MeV [16]. A similar constrain for the L parameter can be achieved studying the dipole polarizability [17] thanks to the measurements performed with the Pb target. The results of these promising investigations are still under analysis and will be presented in forthcoming publications.

Acknowledgments

This experiment was performed within the FAIR Phase-0 beam-time. The work has been supported by the Spanish Ministry for Science and Innovation under grants No. PGC2018-099746-B-C21, PGC2018-099746-B-C22, PID2019-104390GB-I00, PID2021-125771NB-C21, and PID2021-125771NB-C22, by the Regional Government of Galicia under the program "Grupos de Referencia Competitiva" ED431C-2021-38, by the "María de Maeztu" Units of Excellence program MDM-2016-0692, by the German Federal Ministry of Education and Research (BMBF, project 05P2015RDFN1) and by the GSI-TU Darmstadt cooperation agreement. J.L.R.-S. is thankful for support from Xunta de Galicia grant No. ED481D-2021-018. I.G, I.L., D.J.M. have been supported by Croatian Science Foundation (HRZZ) under porject numbers IP-2018-01-1257 and CEMS at RBI.

References

[1] L. Lapikás et al., Nuclear Physics A **553**, 297 (1993)
[2] B.P. Kay et al., Phys. Rev. Lett. **111**, 043502 (2013)
[3] A. Gade et al., Phys Rev. C **90**, 057602 (2014)
[4] J. Díaz-Cortés et al., Phys. Lett. B **811**, 135962 (2020)
[5] V. Vaquero et al., Physics Letters B **795**, 356 (2019)
[6] M. Duer et al., Nature **560**, 617 (2018)
[7] C. Louchart et al., Phys. Rev. C **83**, 011601 (2011)
[8] V. Vaquero et al., Phys. Rev. Lett. **118** 202502 (2017)
[9] H. Alvarez-Pol et al., Nucl. Instrum. Methods A **767**, 453 (2014)
[10] M. Heil et al., Eur. Phys. J. A **58**, 248 (2022)
[11] K. Boretzky et al., Nucl. Instrum. Methods Phys. Res. A **1014**, 165701 (2021)
[12] X. Roca-Maza et al., Phys. Rev. Lett. **106**, 252501 (2011)
[13] J. Hirtz et al., Phys. Rev. C **101**, 014608 (2020)
[14] J. L. Rodríguez-Sánchez et al., Phys. Rev. C **105**, 014623 (2022)
[15] J.-J. Gaimard et al., Nucl. Phys. A **531**, 709 (1991)
[16] T. Aumann et al., Phys. Rev. Lett. **119**, 262501 (2017)
[17] X. Roca-Maza et al., Phys. Rev. C **92**, 064304 (2015)